Journal of the European Ceramic Society 19 (1999) 2297–2303

PII: S0955-2219(99)00117-X
0955-2219/99/$ - see front matter

Interfacial Behavior of Microcomposites During Creep at Elevated Temperatures

Kevin L. Rugg, [a]* Richard E. Tressler [a] and Jacques Lamon [b]

[a]Department of Materials Science and Engineering, The Pennsylvania State University, University Park, PA 16802, USA
[b]Laboratoire des Composites Thermostructuraux, Domaine Universitaire, 33600 Pessac, France

Abstract

The high temperature interfacial behavior of SiC/C/SiC microcomposites was investigated. The interfacial sliding resistance dropped slightly from a room temperature value of 10 MPa with increasing temperature up to 1300°C in argon. The interfacial shear stress was shown to remain constant during the creep of microcomposites at 1200–1300°C and 200–450 MPa in argon. For creep in air, the interfacial shear stress increases at long exposure times. © *1999 Elsevier Science Ltd. All rights reserved.*

Keywords: composites, interfaces, coating, creep, SiC.

1 Introduction

Ceramic matrix composites (CMCs) are being designed for use in high temperature structural applications such as adiabatic engines, heat exchangers, and gas turbines. The temperature dependence of the stress of the fiber/matrix interface, including the effect of creep exposure, has not been well studied. Lamon *et al*. proposed a test procedure using microcomposites to investigate the mechanical behavior of interfaces.[1] A microcomposite (shown in Fig. 1) consists of a single fiber coated by chemical vapor deposition (CVD) with a thin carbon interfacial layer followed by a silicon carbide matrix layer in a method analogous to the processing of chemical vapor infiltrated (CVI) composites. The microcomposite, therefore, represents the basic structural unit of composites. The methodology for determining the interfacial strength involves conducting unload–reload loops following the initiation of matrix cracks.[2,3] The widths of the obtained hysteresis loops are inversely proportional to the interfacial strength.

Lamon *et al*.[2] used the microcomposite test procedure to evaluate the room temperature interfacial properties of SiC/BN/SiC (Nicalon) and SiC/C/SiC microcomposites manufactured by the same processing route as the microcomposites in the present study. The sliding resistances were generally less than 10 MPa with a large spread. Morscher *et al*.[4] and Kerans *et al*.[5] demonstrated the accuracy of the interfacial properties determined from microcomposite by comparing the results with those from pushout tests on identical materials. Morscher *et al*. tested CVD SiC fiber microcomposites with C and BN interfaces and thick (130–160 μm) SiC matrix sheaths while Kerans *et al*. studied Nicalon fiber based microcomposites with a BN interface and SiC matrix. Both studies found good agreement between the two test types. Fernandez and Morscher[6] used the microcomposite test procedure to investigate mechanical behavior up to 1200°C. They determined that the interfacial strength decreased from 10 MPa at room temperature to 2·6 MPa at 470°C. At higher temperatures they could not determine the interfacial strength because of "fatigue" effects on the hysteresis loops. In the present study we report on CVI SiC matrix/C/Hi Nicalon microcomposites tested at temperatures up to 1400°C. Interfacial properties were determined from stepped temperature tests and as a function of creep exposure.

2 Experimental Procedure

The single fiber microcomposites were produced at the Laboratoire des Composites Thermostructuraux (LCTS) in Bordeaux, France using a process similar to that for manufacturing CVI composites.[1] The polymer-derived Hi Nicalon™ SiC-based fiber (Nippon Carbon Company) and

*To whom correspondence should be addressed at: Rockwell Science Center, 1049 Camino Dos Rios, Thousand Oaks, CA 91361, USA.

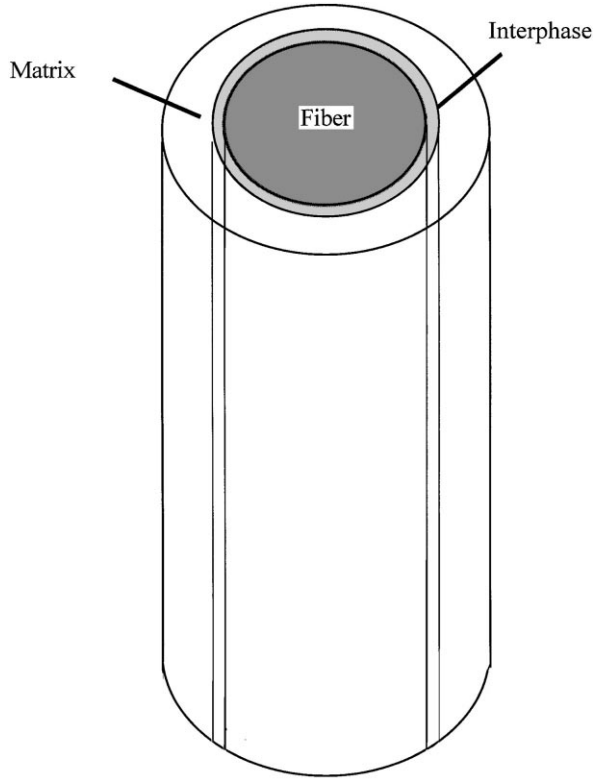

Fig. 1. Schematic of a microcomposite.

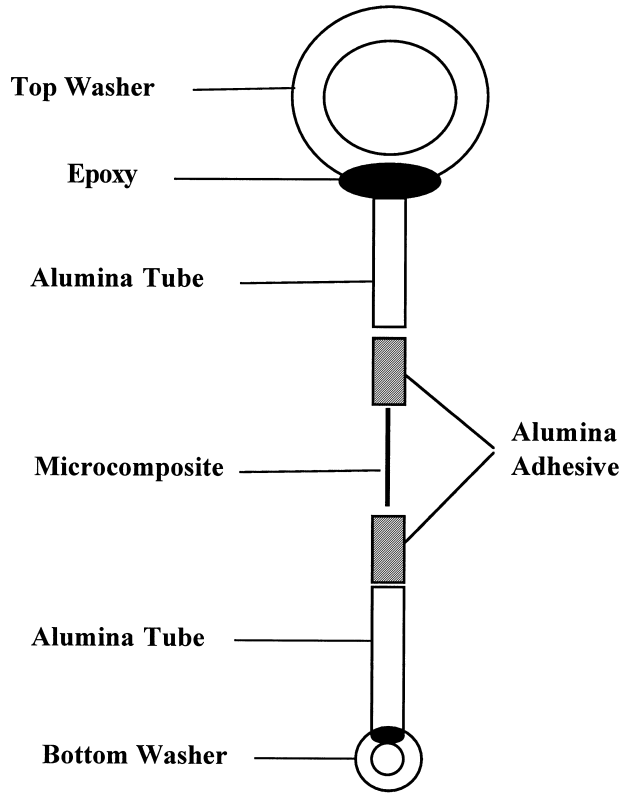

Fig. 2. Schematic specimen gripping arrangement.

the Carborundum polycrystalline SiC fiber (the Carborundum Company) were used. All microcomposites were fabricated with a 0·1 μm pyrocarbon interlayer. The Hi Nicalon microcomposites were received in four batches. The first received in May 1995, designated with the prefix "H5", had a matrix thickness of 5 μm, the second received in May 1996 had a matrix thickness of 10 μm and is designated "H10", and the third and fourth batches received in August 1996 had a 3 μm matrix and are designated "H3". The H5- and H10- batches of microcomposites were fabricated by conventional CVD(CVI) while the H3- batch was prepared by pulsed CVD. The Carborundum fiber microcomposites were fabricated with the H5 Hi Nicalon microcomposites and are designated with a "C" prefix.

Most of the microcomposites (including all those for high temperature experiments) were gripped by cementing them into alumina tubes using an alumina-based adhesive (Aremco Ceramabond 503) as shown in Fig. 2. The 203 μm inner diameter tubes were shaved along 10 mm of their length to expose the microcomposites for application of the adhesive. The specimen length between tubes was 15 ± 1 mm, equivalent to the hot zone of the furnace, ensuring that the matrix cracking and interfacial sliding observed occurred at the temperature of interest. The tubes were epoxied to steel washers for gripping outside the furnace. A few room temperature experiments were conducted by epoxying the microcomposites directly to the washers without use of the alumina tubes to allow gauge lengths of 70–90 mm. Experiments were performed on a fiber testing apparatus designed and built at Penn State.[7] The sample was suspended from a micropositioning motor, through a platinum/rhodium wound tube furnace, to a load cell. Load–unload–reload loops were conducted at stressing rates ranging from 5 to 20 MPa/s. An encoder in the motor monitored the rotations of the drive gear which was converted to specimen displacement. Before high temperature tests, the microcomposites were precracked either in tension or bending at room temperature. This procedure ensured that a sufficient number of matrix cracks was generated under conditions where creep fatigue of the fiber was not significant. The entire test system was encased in a glass bell jar to allow testing in controlled atmospheres. Unless otherwise indicated, experiments were conducted in flowing argon. Due to thermal expansion effects, the apparatus required a 4 h dwell at temperature prior to the commencement of creep experiments.

Matrix crack density and fiber volume fraction were determined by SEM following mechanical testing. For some room temperature tests, the sample was removed from the testing apparatus following each hysteresis loop and inspected by optical microscopy. It was necessary to apply a load to the microcomposite during microscopy to detect the matrix cracks. In this manner, the number of

cracks could be measured for a single microcomposite at a number of peak stresses.

3 Results and Discussion

The stress–displacement curves at room temperature for several microcomposites are shown in Fig. 3. The differences in slope at low stresses for the different samples arise from differences in composite stiffnesses due to differences in sample diameter. The behavior depends on the fiber type and the matrix layer thickness. Microcomposite C-1 is based on the Carborundum SiC fiber and shows linear elastic behavior to failure as did all of the Carborundum microcomposites in this study. For samples with large matrix thickness and small fiber volume fraction, V_f, such as H10-2 ($V_f = 0{\cdot}15$) and H10-3 ($V_f = 0{\cdot}2$) shown in the figure, the fiber stresses near a matrix crack at crack initiation are 5·2 and 3·3 GPa, respectively. The fibers cannot sustain these loads, and the microcomposites fractured. Thus, only linear elastic behavior can be seen.

Microcomposite H10-8 is an exception from this behavior for the H10 series of microcomposites since that specimen had been precracked in bending prior to the tensile test. As a result, H10-8 displays a lower effective elastic modulus than the other microcomposites, a lower peak far field strength, and inelastic behavior. A deviation from linearity can be seen for microcomposites H3-2A, H3-2C, and H3-6B at high stresses. The load drops seen in some of the stress-displacement curves are not necessarily indicative of matrix cracking. Such load drops have been seen during single fiber tensile tests also and could be related to noise in the load reading or a shifting of the sample in the grips.

The matrix cracking stress, σ_{mc}, can be estimated from the stress–strain curve at the first deviation from linear elastic behavior. As can be seen in Fig. 3, the nonelastic displacement typically begins at applied stresses between 500 to 1000 MPa. The matrix cracking stress can be calculated from

$$\sigma_{mc} = \frac{a\sigma_{\text{app}}}{(1 - V_f)(1 + a)} \tag{1}$$

where σ_{app} is the applied stress at matrix cracking, and

$$a = \frac{E_m(1 - V_f)}{E_f V_f} \tag{2}$$

with E_m and E_f the elastic moduli of the matrix (400 GPa) and the Hi Nicalon fiber (280 GPa), respectively.[10] Lamon *et al.*[2] monitored the acoustic emission signal during testing of Nicalon-based microcomposites prepared in the same manner as the microcomposites in the present study. The first matrix cracking stress was 300–1000 MPa with an average of 589 MPa and a Weibull modulus of 4·9 for 10 mm long samples,[8] consistent with the onset of nonlinearity for the current microcomposites.

The properties of the fiber/matrix interface can be determined using unload–reload hysteresis loops conducted at peak stresses greater than the matrix cracking stress. The sliding resistance, τ, can be determined from the hysteresis loop width, $\delta\Delta$, using

$$\tau = \frac{b_2 N(1 - a_1 V_f)^2 \sigma_p^2 R(\sigma/\sigma_p)[1 - \sigma/\sigma_p]}{2E_m V_f^2 \delta\Delta} \tag{3}$$

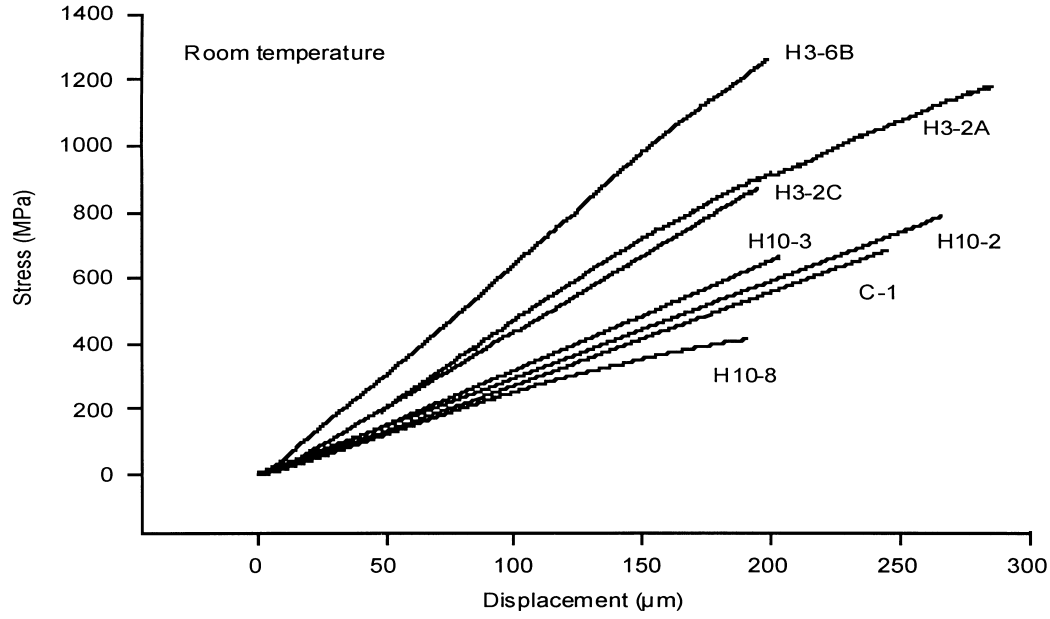

Fig. 3. Typical stress-displacement behavior during load up for microcomposites at room temperature.

where σ_p is the peak stress, N is the number of matrix cracks, R is the fiber radius, σ is the stress at which $\delta\Delta$ is measured, and b_2 and a_1 are dimensionless constants determined from the elastic constants and volume fractions of the fiber and matrix as given in Ref. 9.

The hysteresis results for several Hi Nicalon based microcomposites at room temperature are given in Table 1. (Hysteresis was never seen for Carborundum microcomposites.) Since the number of matrix cracks is not known for all samples listed, the results are reported as τ/N and converted to τ when possible. Sample H5-1 was removed after each hysteresis loop and examined for matrix crack density by optical microscopy. An example of an hysteresis loop for this sample is given in Fig. 4. The calculated value of τ following the final hysteresis loop of 9.8 MPa is comparable to the τ/N values for microcomposites H5-10 and H10-9 assuming they had just one crack each and for the rest of the microcomposites listed for 2–5 matrix cracks. The results are similar to those reported in Ref. 8 for Nicalon microcomposites where τ ranged between 4·5 and 6 MPa and 2–5 cracks were typically detected along 10–25 mm gauge lengths.

The high temperature interfacial behavior was determined using the same hysteresis loop technique as was used at room temperature. The analysis of the high temperature loops was complicated by creep of the composite. Equation 1 was derived for elastic load sharing conditions which are not met at elevated temperatures when creep processes are active. During the high stress portion of the hysteresis loops, load is quickly shed from the less creep resistant matrix to the fiber.[10] At the low stress part of the hysteresis loop the reverse behavior occurs. The hysteresis loop shape is affected by the creep processes, resulting in loops that do not close properly at the top. Two different effects can be seen depending at what point of the sample's creep history the hysteresis loop takes place. Early in the creep test, the creep rate is very high and the microcomposite creeps at virtually all applied stresses to allow relaxation of stresses arising during load up from elastic modulus mismatch. This effect results in reload curves which cross the unload curve at a stress lower than σ_p. This effect may be related to the 'fatigue' of the hysteresis loops reported by Fernandez and Morscher[6] for microcomposites at temperatures greater than 500°C. Later in the creep tests, the microcomposites do not creep at all stress levels and recovery occurs during the low stress portions of the hysteresis loops. Recovery causes the fiber stress to be lower after the unload–reload cycle than it was before the cycle. This results in a lower strain following the cycle, since a portion of the previously accumulated elastic strain is absent. Therefore, these hysteresis loops do not close. To limit the creep effects, the hysteresis loops were run at strain rates as fast as practical. Hysteresis loop widths were also measured at lower applied stresses ($\sigma_p/4$) as a check on the results at half-maximum so that the stress states on both sides of the hysteresis loops would be as close as possible.

The τ/N values calculated from a stepped temperature test are shown in Fig. 5. Hysteresis loops were performed at increasing temperatures up to 1400°C then reduced, as indicated in the plot. Failure occurred upon loading at 1100°C. The peak stress was 572 MPa. It can be seen that τ/N

Table 1. Results of hysteresis tests at room temperature for Hi Nicalon microcomposites[a]

Sample[a]	V_f	σ_p *(MPa)*	$\delta\Delta$ *(1/2 max)* μm	τ/N *(MPa)*	*N*	τ *(MPa)*[c]
H3-1	0·45	1000	0·66	7·4	1	7·4
H3-5A	0·48	1000	1·96	1·4	20?	28?
H3-7A	0·51	1000	2·07	2·1		
H3-7B	0·51	900	1·78	2·0	7	13·8
H5-1	0·36	360	3·27	0·49		
		369	8·41	0·23		
		432	15·08	0·15		
		432	13·77	0·16		
		468	19·33	0·14	37	5·1
		400	18·87	0·10	57	5·8
		500	24·72	0·12	80	9·8
H5-5	0·47	1048	2·93	2·44		
		572	1·11	1·92		
H5-10	0·28	500	0·63	8·9	1	8·9
H10-9[b]	0·20	426	1·05	9·1	6	54·6
H10-10[b]	0·17	350	1·79	5·5		
H10-11[b]	0·17	335	1·54	6·0		

[a]Gauge length 14–15 mm except H5-1 which had a gauge length of 72–74 mm.

[b]Precracked in bending.

[c]τ Calculated using $E_m = 400$ GPa, $E_f = 280$ GPa, $\nu = 0{\cdot}17$, $E = V_f E_f + (1 - V_f)E_m$.

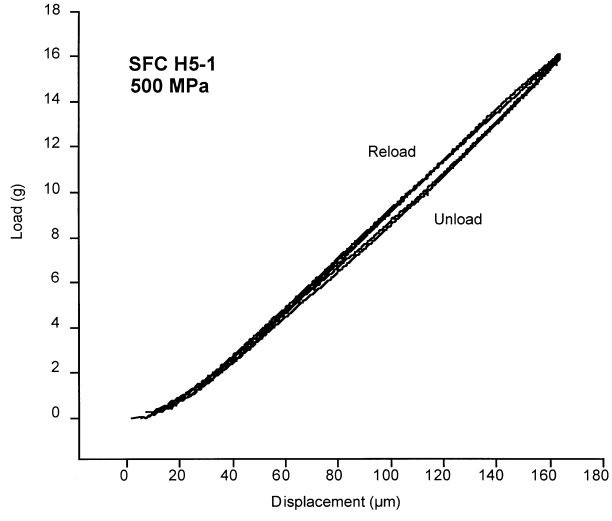

Fig. 4. The 500 MPa hysteresis loops (2) of microcomposite H5-1.

decreases as the temperature increases. The sample was not removed from the rig between temperatures, so it is unknown if the number of matrix cracks was the same at all test temperatures. It has been demonstrated that the matrix of these microcomposites degrades significantly at temperatures $\geq$1300°C.[11] It is evident that the microcomposites weakened as a result of their exposure to stress and temperature.

Creep tests of microcomposites were periodically interrupted by hysteresis loops to determine the effect of creep exposure on the interfacial properties. Figure 6 shows a series of hysteresis loops conducted on a microcomposite at different times during creep at 1250°C and 436 MPa. The initial loop shows a large creep effect as described earlier with the reload curve crossing the unload curve well below σ_p. It can be seen that the loops stay parallel to each other over time; there is no distinct change in the elastic modulus of the microcomposite. This observation is true for all of the microcomposites tested, indicating that the number of cracks did not change tremendously during creep and that the debond length remained quite constant (small growth of the interfacial crack). It can also be seen that the hysteresis loops have roughly the same width, although the 8 h loop for the sample shown in the figure (taken 20 min before failure of the microcomposite) does appear to be slightly wider.

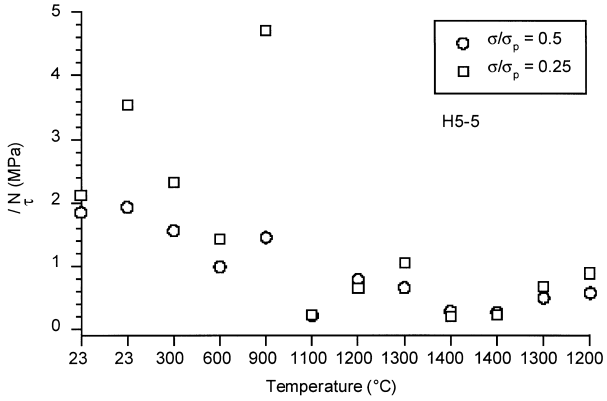

Fig. 5. Interfacial strength measured from hysteresis loop experiments during temperature change tests for a Hi Nicalon microcomposites.

The hysteresis loop widths and calculated shear stresses during creep for a number of microcomposites are given in Table 2. The creep curves for these samples are presented elsewhere.[10] The data for sample H3-8 represent the average loop width for multiple loops at each time step. There are differences in the results depending on the σ/σ_p ratio at which the analysis was conducted and between consecutive loops when multiple loops were run at each time interval. Some of the results seem to indicate a decrease in interfacial stress over time, but this decrease is insignificant considering the scatter in the measurements. A decrease in τ may result from growth of the fiber/matrix interface, from the creep of the microcomposite constituents, or be a product of the method used for the τ determination. However, the τ decrease may have resulted from fiber stretching during creep which locally affects the fiber/matrix interactions. The values of the interfacial stress during creep are slightly lower than those measured at room temperature, but again within the extent of the scatter.

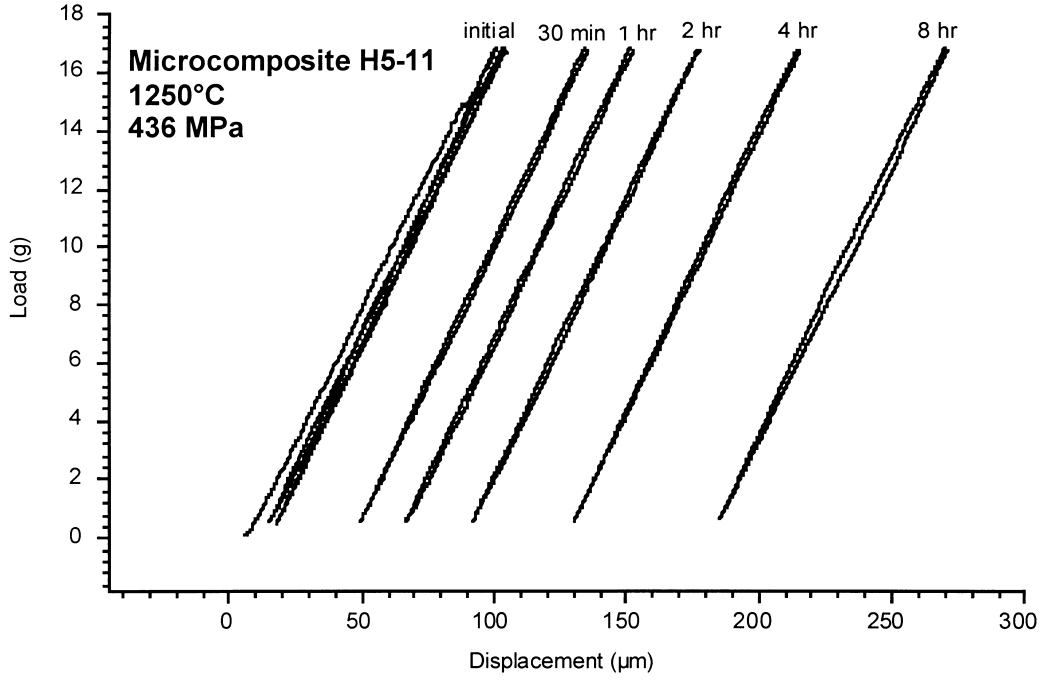

Fig. 6. Series of hysteresis loops for microcomposite H5-11 at different times during creep at 1250°C and 436 MPa in argon.

The near constancy of τ values is consistent with the results of a micromechanical model for the creep of microcomposites with matrix cracks.[10] In that model, the interfacial shear stress quickly decreases from 10 to 7 MPa within 30 min of creep at 1300°C and 300 MPa, after which it remains steady. Since the hysteresis loops conducted during the first stages of the creep test are often difficult to interpret, the initial drop off in interfacial shear stress predicted by the model is not observed experimentally.

The small variation of the interfacial behavior during creep is markedly different from the observations of previous authors. Lamouroux *et al.*[12] observed a weakening of the interface of an Al_2O_3 fiber reinforced SiC composite which they suggested was due to progressive debonding of the interface. Evans and Weber[13] investigated a 2D SiC/SiC composite. The hysteresis loops conducted became wider and the elastic modulus decreased over time. Matrix cracks from the 90° plies propagated subcritically across the 0° plies causing the decrease in properties. For the microcomposites in the present study, neither progressive debonding nor increased matrix damage is observed.

While there was only a minor change in the interfacial shear stress due to creep exposure, the matrix crack opening did change appreciably in a number of instances. Figure 7 shows the SEM micrograph of a typical room temperature matrix crack resulting from a monotonic test compared to a matrix crack from sample H10-9 which had crept at 1300°C and 199 MPa for 24 h. All room temperature (and many high temperature) cracks were closed, but the crack shown in Fig. 7 widened to approximately 13 μm due to creep of the fiber at the crack opening.

The results of hysteresis tests conducted during creep of a microcomposite in air at 1200°C is shown in Fig. 8. For the first 6 h, the interfacial shear stress does not change. At longer times, the hysteresis loop widths close significantly and the value of τ increases. This interfacial strengthening is most likely caused by oxidative closing of the

Table 2. Hysteresis loop widths and calculated interfacial shear stress as a function of time during creep tests

		$\sigma/\sigma_p = 0{\cdot}25$		$\sigma/\sigma_p = 0{\cdot}5$	
Sample	*Creep time (h)*	$\delta\Delta$ (μm)	τ/N (MPa)	$\delta\Delta$ (μm)	τ/N (MPa)
H10-9	1	0·11	13·7	0·72	2·8
1300°C	2	1·46	1·0	2·02	1·0
199 MPa	5	0·31	4·9	–	–
6 cracks	9·8	0·25	6·0	0·41	4·9
$V_f = 0{\cdot}20$	20	0·58	2·6	1·34	1·5
	24	1·30	1·5	1·98	1·0
H5-9	0	1·35	2·0	2·21	1·6
1300°C	0·5	2·53	1·1	3·65	1·0
381 MPa	1	1·39	1·9	1·18	1·1
3 cracks	2	1·87	1·4	1·68	1·0
$V_f = 0{\cdot}27$	4	1·96	1·4	4·47	0·8
	8	2·53	1·1	3·94	0·9
H5-10	0·5	0·66	2·4	0·70	3·0
1200°C	1	0·28	5·6	0·73	2·9
305 MPa	2	0·47	3·3	0·24	8·7
$V_f = 0{\cdot}28$					
375 MPa	2	0·69	3·4	2·00	1·6
	2·5	0·11	21·5	0·94	3·4
1 crack	3	–	–	0·25	0·29
H5-11	0	1·64	2·0	1·23	3·5
1250°C	0·03	0·86	3·7	0·94	4·5
436 MPa	30	1·39	2·3	2·03	2·1
2–4 cracks	1	1·85	1·7	1·70	2·5
$V_f = 0{\cdot}37$	2	1·38	2·3	1·75	2·4
	4	0·90	3·6	1·56	2·7
	8	1·28	2·5	3·17	1·3
H3-8[a]	0	2·55	0·25	2·68	0·32
1200°C	1	0·94	0·67	1·66	0·51
450 MPa	2	0·81	0·78	2·59	0·33
21 cracks	4	2·28	0·28	4·03	0·21
$V_f = 0{\cdot}50$	10	1·62	0·39	3·44	0·25
	24	0·54	1·17	0·89	0·95

[a]Loop width average of 3–4 consecutive loops.

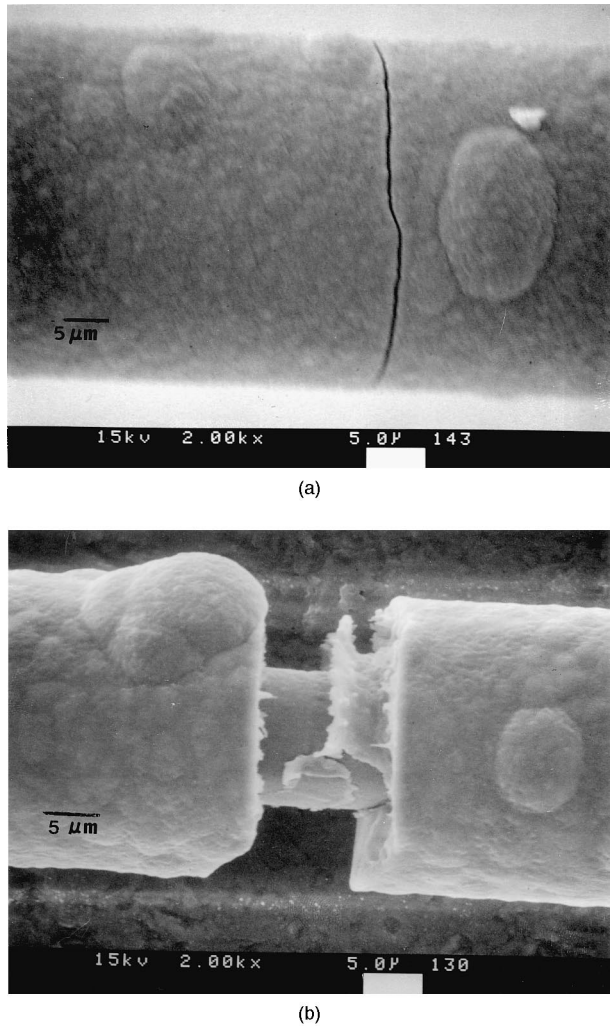

Fig. 7. (a) A typical room temperature matrix crack. (b) An open matrix crack from a creep specimen.

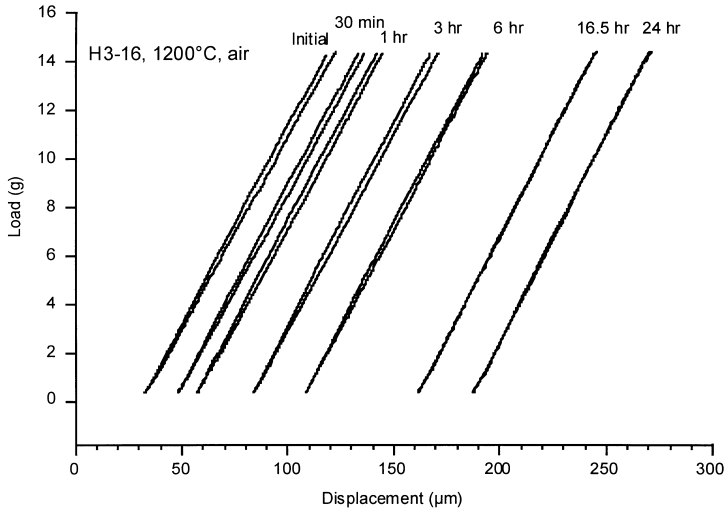

Fig. 8. Hysteresis loops for sample H3-16 crept at 486 MPa and 1200°C in air showing the decrease of hysteresis loop width at long times.

matrix crack and/or the fiber/matrix interface. Oxidation results in the formation of a glass which increases the fiber/matrix interaction.

4 Summary

The strength of the fiber/matrix interface of SiC/C/SiC microcomposites has been evaluated over a temperature range of 25–1400°C as a function of temperature and creep exposure. It was found that the sliding resistance decreased slightly with increasing temperature from an initial value of approximately 10 MPa at room temperature. The hysteresis loop width and interfacial shear stress decreased slightly during creep in argon. During creep in air, the interfacial shear stress increased significantly following creep exposures over 8 h.

Acknowledgements

Supported by the NASA HITEMP Program. Cooperation between PSU and LCTS was supported by NSF and CNRS.

References

1. Lamon, J., Rechiniac, C., Lissart, N. and Corne, P., Determination of interfacial properties in ceramic matrix composites using microcomposite specimens. In *Proceedings of the 5th European Conference on Composite Materials*, ed. L. Bunsell. EACM-CEC, Bordeaux, France, 1992, p. 585.
2. Lamon, J., Rebillat, F. and Evans, A. G., Microcomposite test procedure for evaluating the interface properties of ceramic matrix composites. *J. Am. Ceram. Soc.*, 1995, **78**(2), 402–405.
3. Vagagginni, E., Domergue, J. M. and Evans, A. G., Relationships between hysteresis measurements and the constituent properties of ceramic matrix composites: I, theory. *J. Am. Ceram. Soc.*, 1995, **78**(10), 2709–2720.
4. Morsher, G. N., Fernandez, J. M. and Purdy, M. J., Determination of interfacial properties using a single fiber microcomposite test. *J. Am. Ceram. Soc.*, 1996, **79**(4), 1083–1091.
5. Kerans, R. J., Rebillat, F. and Lamon, J., Fiber–matrix interface properties of single-fiber microcomposites as measured by fiber pushin tests. *J. Am. Ceram. Soc.*, 1997, **80**(2), 506–508.
6. Fernandez, J. M. and Morscher, G. N., Determination of interfacial properties in function of temperature using a single fiber microcomposite test. In *In High Temperature Ceramic-Matrix Composites I.*, ed. A. G. Evans and R. Naslain. American Ceramic Society, Westerville, OH, 1995, pp. 279–284.
7. Pysher, D. J., Giannuzzi, L. A. and Tressler, R. E., An apparatus for mechanically testing single filaments at high temperature in a controlled atmosphere or vacuum, submitted to *Rev. Sci. Instruments*.
8. Lamon, J., Lissart, N., Rechiniac, C., Roach, D. H. and Jouin, J. M., Micromechanical and statistical approach to the behavior of CMC's. *Cer. Eng. Sci. Proc.*, 1993, **14**(9–10), 1115–1124.
9. Hutchinson, J. W. and Jensen, H. M., Models of fiber debonding and pullout in brittle composites with friction. *Mech. Mat.*, 1990, **9**, 139–163.
10. Rugg, K. L., Tressler, R. E. and Lamon, J., Creep of SiC–SiC microcomposites. *J. Euro. Ceram. Soc.*, 1999, **19**(13–14), this issue.
11. Rugg, K. L. Tressler, R. E. Pailler, R. and Lamon, J., Creep of CVI silicon carbide matrix for composites. submitted to *J. Am Ceram. Soc.* 1997.
12. Lamouroux, F., Steen, M. and Vallés, J. L., Uniaxial tensile and creep behaviour of an alumina fibre-reinforced ceramic matrix composite: I. Experimental study. *J. Euro. Ceram. Soc.*, 1994, **14**, 529–537.
13. Evans, A. G. and Weber, C., Creep Damage in SiC/SiC Composites. *Mat. Sci. Eng. A*, 1996, **A208**, 1–6.